Jellium work function for all electron densities

John P. Perdew and Yue Wang
Department of Physics and Quantum Theory Group, Tulane University, New Orleans, Louisiana 70118
(Received 7 March 1988)

The work function and surface energy of jellium have been calculated for low ($r_s=12$), metallic ($2\le r_s\le 6$), and high ($0.5\le r_s\le 2$) bulk electron densities. As the density increases, the work function peaks at 3.8 eV ($r_s=1.7$), minimizes at 3.6 eV ($r_s=0.9$, a density higher than that of metastable metallic hydrogen), peaks again at 3.7 eV ($r_s=0.6$), and finally drops toward a high-density limit around 2.0 eV ($r_s\to 0$). The self-consistent calculations, which employ an accurate electron-gas exchange-correlation energy within the local-density approximation, are numerically challenging at high densities. Exchange-only calculations, which display the same double-peaked density dependence, are also reported. The high-density limits for the work function with and without correlation (2.0 and 1.0 eV, respectively) have been estimated in two ways: (1) from an extension of Peuckert's argument, and (2) from the Thomas-Fermi-Dirac-Gombas approximation.

I. INTRODUCTION AND SUMMARY OF CONCLUSIONS

This study extends the jellium-surface calculations of Lang and Kohn[1,2] beyond the normal range of metallic densities, with special attention to the high densities attainable by metals under pressure. In the jellium model, the positive ions are replaced by a uniform background of positive charge density

$$\bar{n}=3/4\pi r_s^3=k_F^3/3\pi^2 . \quad (1)$$

(All equations are in atomic units, where $\hbar=m=e^2=1$.) This background fills the half-space $x<0$ and is neutralized by the electron density $n(x)$. Using the local-density approximation for exchange and correlation,[3] Lang and Kohn self-consistently calculated $n(x)$ as well as the surface energy and work function in the range of metallic densities, $2\le r_s\le 6$. They found that the jellium model predicts work functions close to those measured for real *sp*-bonded metals, including the alkalis and simple polyvalents. In these simple metals, the work function ranges roughly from 2 eV at $r_s\approx 6$ to 4 eV at $r_s\approx 2$. Transition metals $[(3d)^n(4s)^m]$ display higher average valence electron densities ($r_s\approx 1.3$), but the jellium model is inappropriate to such highly-nonuniform bulk densities.

Still higher densities may be sampled by materials under pressure. If the external pressure is suddenly released, the material is left in an unstable or metastable compressed state. The mobile electrons at the surface can presumably relax before the nuclear positions do. For example,[4] metallic hydrogen is predicted to have a metastable phase at some density in the range $1.0\le r_s\le 2.0$.

Recently Magaña and Ocampo[4] calculated a work function of 4.67 eV for jellium at $r_s=1$, representing metallic hydrogen. Instead of making a fully self-consistent calculation, they varied a trial input Kohn-Sham effective potential $v_{\rm eff}(x)$ until the input and output potentials were similar. Although Magaña and Ocampo reproduced the Lang-Kohn work function to within 0.1 eV at $r_s=2$, their procedure is not necessarily that accurate at higher densities where the work function is the residue of a delicate cancellation. Our own calculations, which we believe are fully self-consistent, yield a jellium work function of 3.60 eV at $r_s=1$. (Sahni has informed us of his elaborate unpublished variational calculation with Ma, which yields 3.5 eV at $r_s=1$, and work functions virtually identical to ours for $r_s\ge 2.5$.)

Our local-density calculations employ a parametrization[5] of the Ceperley-Alder[6] correlation energy $\varepsilon_c(n)$ for the electron gas of uniform density n. The Ceperley-Alder $\varepsilon_c(n)$ is more accurate than the Wigner form used by Lang and Kohn, or the Hedin-Lundqvist form used by Magaña and Ocampo (for which we find $W=3.68$ eV at $r_s=1$.) Table I lists our results for the work function W and surface energy σ of jellium in the range $0.5\le r_s\le 12$, while Fig. 1 graphs W versus r_s. An unexpected feature is the shallow minimum in W at $r_s=0.9$ In Sec. II we describe how our calculations were performed and explain why they become numerically challenging at high density. At the end of that section, we attempt to explain the double-peaked density dependence of the calculated work function.

A by-product of this work is the first careful *numerical* demonstration of the equivalence of the exact expressions (8) and (9) for the work function.

We have found no reliable self-consistent solution for $r_s<0.5$. What then is to be expected in the high-density ($r_s\to 0$) limit? Peuckert[7] argued that the work function should tend to a finite constant, which he estimated to be 1.2 eV. In this limit, the work function is determined largely by a tail of metallic or low-electron density lying 5 bohr or further outside the jellium edge ($x=0$). Peuckert's estimate results from matching the image-potential behavior $W-1/4x$ far outside the surface to the high-density expansion of $v_{\rm eff}(x)-\mu$. Here $\mu=-W+v_{\rm eff}(\infty)$ is the chemical potential, and $v_{\rm eff}(x)$ is

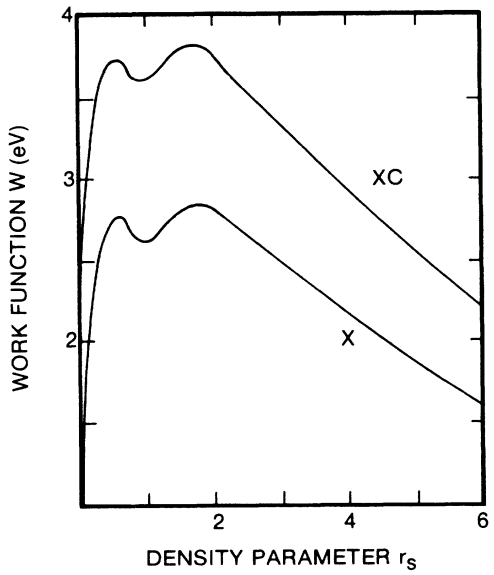

FIG. 1. Density dependence of the work function of jellium, within the local-density approximation. *X*, exchange-only; *XC*, exchange and correlation. For $r_s \geq 0.5$, the curves have been plotted from the self-consistent calculations of Table I. For $r_s < 0.5$, they have been extrapolated toward our estimated high-density limits.

the Kohn-Sham effective potential, which Peuckert evaluated within the local-density approximation for exchange (neglecting correlation).

Peuckert's derivation needs to be improved in two ways. (1) The asymptotic behavior within the exchange-only local-density approximation is not $W-1/4x$ but $W-[3\pi^2 n(x)]^{1/3}/\pi$. We make this correction in Appendix A, obtaining 1.0 eV as the high-density limit of the exchange-only work function. (2) According to our self-consistent results in Table I, correlation contributes about 1.0 eV to the work function for small r_s. Thus our best estimate for the high-density limit of the work function, including correlation, is 2.0 eV.

Some insight into the high-density limit may be gleaned from the Thomas-Fermi (TF), Thomas-Fermi-Dirac (TFD), and Thomas-Fermi-Dirac-Gombas[8] (TFDG) approximations. All three involve a local-density approximation for the *kinetic* energy, which is valid when the electron density varies slowly over the local Fermi wavelength $\lambda_F = 2\pi/k_F = 3.27 r_s$ (i.e., when $|\nabla n|/2k_F n \ll 1$). Since the characteristic decay length of the jellium surface is the Thomas-Fermi screening length $k_s^{-1} = (4k_F/\pi)^{-1/2} = 0.64 r_s^{1/2}$, the condition of slow density variation is most nearly achieved in the high-density limit. As demonstrated in Appendix B, the TFD value for the density ratio $n(0)/\bar{n}$ is realistic for high bulk density $\bar{n}$, and unrealistic for low. Similarly, the relative error of any TF-based value for the electrostatic surface dipole barrier approaches zero in the high-density limit.

Within the TF approximation, which neglects both exchange and correlation, the work function of jellium is identically zero. Within the TFD approximation, which includes exchange, the work function is 1.3 eV, independent of the bulk density. Within the TFDG approximation, which incorporates correlation as well, the work function is 2.1 eV. These values were first obtained by Smith,[9] following an argument due to Sheldon[10] which is outlined in Appendix B of this paper. We propose that the TFDG and TFD work functions are estimates of the high-density limits with and without correlation, respectively.

II. SELF-CONSISTENCY PROCEDURE

Our self-consistent local-density calculations for the jellium surface have been made with an enhanced version of the Monnier-Perdew computer code.[11] As in the

TABLE I. Density dependence of the work function *W*, surface dipole barrier $\Delta\phi = \phi(\infty) - \phi(-\infty)$, and surface energy σ within the local-density approximation. *X*, exchange only; *XC*, exchange and correlation. $r_s = (3/4\pi\bar{n})^{1/3}$ is the bulk density parameter. (1 hartree = 27.21 eV, 1 hartree/bohr^2 $= 1.556\,92 \times 10^6$ ergs/cm^2.) For purposes of interpolation or fitting at small r_s, the most useful quantities to consider are $(\Delta\phi) r_s^2$ and $(\sigma) r_s^{9/2}$. The last significant figure is usually the last nonzero digit.

	W (eV)		$\Delta\phi$ (eV)		σ (ergs/cm^2)	
r_s	*X*	*XC*	*X*	*XC*	*X*	*XC*
0.50	2.73	3.71	169.93	168.58	−2 140 250	−2 123 730
0.625	2.77	3.73	104.46	103.26	−735 280	−726 300
0.75	2.70	3.66	69.62	68.54	−302 460	−297 040
0.875	2.64	3.60	49.09	48.12	−140 655	−137 140
1.00	2.62	3.60	36.12	35.24	−71 430	−69 026
1.25	2.69	3.69	21.46	20.77	−22 055	−20 782
1.5	2.79	3.80	13.98	13.40	−7911	−7161
2.0	2.81	3.78	7.03	6.59	1186.7	−861.5
3.0	2.50	3.35	2.53	2.21	126.7	224.6
4.0	2.15	2.90	1.13	0.86	122.7	163.4
5.0	1.87	2.54	0.55	0.31	77.4	97.5
6.0	1.63	2.25	0.25	0.04	48.4	59.4
12.0	0.92	1.34	−0.12	−0.25	5.8	6.6

Lang-Kohn calculation,[1] the density $n(x)$ is constructed as the solution of the Kohn-Sham equations:[3]

$$n(x)=\sum_i |\psi_i(\mathbf{r})|^2\Theta(\mu-\varepsilon_i)\ , \tag{2}$$

$$[-\tfrac{1}{2}\nabla^2+v_{\rm eff}(x)]\psi_i(\mathbf{r})=\varepsilon_i\psi_i(\mathbf{r})\ , \tag{3}$$

$$v_{\rm eff}(x)=\phi(x)+\mu_{\rm xc}(n(x))\ , \tag{4}$$

$$\phi(\mathbf{r})=\int d^3r'\frac{n(\mathbf{r}')-n_+(\mathbf{r}')}{|\mathbf{r}'-\mathbf{r}|}\ , \tag{5}$$

$$\mu_{\rm xc}(n)=d[n\varepsilon_{\rm xc}(n)]/dn\ . \tag{6}$$

Here $n_+(\mathbf{r})=\bar{n}\Theta(-x)$ is the density of the positive background, and $\varepsilon_{\rm xc}(n)=\varepsilon_x(n)+\varepsilon_c(n)$ is the exchange-correlation energy per particle in an electron gas of uniform density n. In the Monnier-Perdew code, however, the electrostatic potential $\phi(x)$ is constructed via the solution of an integral equation[11,12] which is iterated along with the density $n(x)$ and effective potential $v_{\rm eff}(x)$. The intended surface charge density

$$\Sigma=-\int_{-\infty}^{\infty}dx[n(x)-\bar{n}\Theta(-x)] \tag{7}$$

(which is zero for a neutral surface) is achieved only at the self-consistency limit, as a result of the boundary conditions[11,13] imposed upon $\phi(x)$. This iteration scheme is stabler and more automatic than the Lang-Kohn scheme in which $\phi(x)$ is obtained directly from Eq. (5).

The work function W may be evaluated via two different expressions which agree only at self-consistency. The change in self-consistent-field expression[13] is

$$W=d\sigma/d\Sigma\ , \tag{8}$$

the derivative of the surface energy σ with respect to the surface charge density Σ, evaluated at $\Sigma=0$. The Koopmans-theorem expression[1,2] is

$$\begin{aligned}W&=v_{\rm eff}(\infty)-v_{\rm eff}(-\infty)-\varepsilon_F(\bar{n})\\&=\phi(\infty)-\phi(-\infty)-\varepsilon_F(\bar{n})-\mu_{\rm xc}(\bar{n})\ ,\end{aligned} \tag{9}$$

where $\varepsilon_F(\bar{n})=k_F^2/2$ is the Fermi energy.

Both expressions for the work function are hard to evaluate accurately for high bulk density $\bar{n}$. In Eq. (8), the surface energy σ diverges like $r_s^{-9/2}$ as $r_s\to 0$,[14] yet its derivative with respect to surface charge density tends to a constant. In Eq. (9) the surface dipole barrier $\phi(\infty)-\phi(-\infty)$ and Fermi energy $\varepsilon_F(\bar{n})$ diverge like r_s^{-2}, the exchange potential $\mu_x(\bar{n})=-k_F/\pi$ diverges like r_s^{-1}, and the correlation potential $\mu_c(\bar{n})$ like $\ln r_s$, yet the self-consistent work function tends to a positive constant in the high-density limit.[7] Incorrect negative divergences have been obtained from restricted variational calculations.[15,16] Thus calculations of the work function at high density must be performed self-consistently and with great care.

Our numerical calculations are performed inside a region extending from $x_0=-3.5\lambda_F$ to $x_1>+0.5\lambda_F$, where $\lambda_F=2\pi/k_F$ is the bulk Fermi wavelength. The outer edge x_1 is increased along with the bulk density to a maximum of $+6\lambda_F$ at $r_s=0.5$. The density $n(x)$ is represented as an asymptotic Friedel oscillation[1] about $\bar{n}$ for $x<x_0$, and as a decaying exponential for $x>x_1$. The integration mesh in real space is extremely fine, with interval $\Delta(x/\lambda_F)=0.001\,25$. Equation (3) is solved by the Numerov method, and all numerical integrations are evaluated with the help of a six-point polynomial rule.

The sum over one-electron quantum numbers i in Eq. (2) may be reduced[1] to a numerical integral over wave number k:

$$n(x)=\frac{1}{\pi^2}\int_0^{k_F}dk(k_F^2-k^2)\,|\psi_k(x)|^2\ , \tag{10}$$

where

$$\psi_k(x)\to\sin[kx-\Gamma(k)] \tag{11}$$

as $x\to-\infty$. At high density, the phase shift $\Gamma(k)$ rises steeply as k approaches k_F, so a fine integration mesh is required, with interval $\Delta(k/k_F)=0.0025$.

Covergence is hastened by optimizing the arbitrary screening parameter K in the integral equation[11,12] for $\phi(x)$. For $r_s\geq 2$, $K\approx k_F$ suffices, but for $r_s=0.5$ convergence is faster with $K\approx 0.6k_F$. Stable self-consistent solutions are obtained after 99 iterations.

We adopt several criteria for a self-consistent solution. (1) The work function and surface energy must be converged with respect to iteration and refinement of integration meshes, and stable under variation of other input parameters. (2) The actual surface charge density must lie within 2×10^{-5} electrons/bohr^2 of the intended surface charge density. (3) The surface dipole barrier computed as $\phi(\infty)-\phi(-\infty)$ must lie within 0.02 eV of the surface dipole moment[1]

$$4\pi\int_{-\infty}^{\infty}dx\,x[n(x)-\bar{n}\Theta(-x)]\ . \tag{12}$$

(4) The Budd-Vannimenus theorem,[17]

$$\phi(0)-\phi(-\infty)=\bar{n}d[\tfrac{3}{5}\varepsilon_F(\bar{n})+\varepsilon_{\rm xc}(\bar{n})]/d\bar{n}\ , \tag{13}$$

must be satisfied to better than 0.01 eV. (5) The work functions computed from expressions (8) and (9) must agree within 0.01 eV. This last criterion is imposed only for $r_s\geq 1$. At higher densities we use only Eq. (9), since the surface energy σ needed in Eq. (8) is not computed to sufficient accuracy.

From these considerations, the numerical error of the computed work function is estimated to be 0.02 eV for $r_s\geq 1$, and a bit larger (possibly 0.04 eV) for $r_s<1$.

The minimum in the calculated work function at $r_s=0.9$ (see Table I or Fig. 1) seems to be too pronounced, too regular, and too reproducible to be an artifact of numerical error. This minimum is not found in a restricted variational calculation of the work function,[15] in which the work function rises with increasing density to a single maximum around $r_s=1.6$, then plunges monotonically to negative values for $r_s<0.8$. The minimum and second maximum found in the present calculation may result from a feature of the self-consistent density that is absent from the restricted variational calculation: The development of a long, Thomas-Fermi-like

$[(x+a)^{-6}]$ tail, which makes an additional contribution to the surface dipole barrier of Eq. (12).

ACKNOWLEDGMENTS

One of us (J.P.) thanks Viraht Sahni and John Smith for helpful correspondence, and Tulane University Computer Services for assistance. This work was supported in part by the National Science Foundation under Grant No. DMR84-20964.

APPENDIX A: PEUCKERT'S HIGH-DENSITY LIMIT

Within the local-density approximation for exchange, the Kohn-Sham effective potential $v_{\rm eff}(x)$ at a distance x outside the jellium edge is

$$v_{\rm eff}(x)-\mu=\phi(x)-\phi(\infty)-(3\pi^2 n)^{1/3}/\pi+W \ . \quad \text{(A1)}$$

Here W is the work function, $\mu=-W+\phi(\infty)$ is the chemical potential, and $\phi(x)$ is the electrostatic potential, which obeys Poisson's equation

$$d^2\phi/dx^2=-4\pi n \ . \quad \text{(A2)}$$

In the high-density limit, (A1) may be expanded as[7]

$$v_{\rm eff}(x)-\mu=-277.5826x^{-4}+2.708\,333x^{-2}+0.007\,419\,275+(6.465\times10^{-5})x^2+\cdots \quad \text{(A3)}$$

According to Peuckert,[7] the first four terms of this expansion suffice for $x\lesssim 14$ bohrs. Expression (A3) diverges as $x\to 0$, but is finite for any positive x. In the high-density limit, the bulk density $\bar{n}=3/4\pi r_s^3$ diverges, as does the density at the jellium edge $[n(0)\to 0.465\bar{n}]$, but the density at any positive x tends to a finite limit because the decay length vanishes like $r_s^{1/2}$.

For very large x (say, $x\gtrsim 14$ bohrs), the electron density decays exponentially:

$$n(x)=\beta\exp(-2\sqrt{2W}x) \ , \quad \text{(A4)}$$

as does the solution of (A2):

$$\phi(x)=\phi(\infty)-4\pi\beta\exp(-2\sqrt{2W}x)/8W \ . \quad \text{(A5)}$$

We seek β, W, and x_m to match $v_{\rm eff}(x)-\mu$, $d[v_{\rm eff}(x)-\mu]/dx$, and $d^2[v_{\rm eff}(x)-\mu]/dx^2$ at $x=x_m$, using expression (A3) for $x\le x_m$ and expressions (A1), (A4), and (A5) for $x\ge x_m$. The result is $\beta=0.002\,06$ bohr^{-3}, $W=0.0367$ hartree $=1.00$ eV, and $x_m=13.15$ bohrs. The computed density at $x=x_m$ is extremely low, corresponding to a local $r_s=52$.

APPENDIX B: THOMAS-FERMI-DIRAC-GOMBAS THEORY OF THE WORK FUNCTION

With a local approximation for the kinetic, exchange, and correlation energies,[8] the total energy functional for jellium is

$$E[n]=\int d^3r\, n(\mathbf{r})\varepsilon(n(\mathbf{r}))+\tfrac{1}{2}\int d^3r\,\phi(\mathbf{r})[n(\mathbf{r})-n_+(\mathbf{r})] \ , \quad \text{(B1)}$$

where $\phi(\mathbf{r})$ is the electrostatic potential of Eq. (5) and

$$\varepsilon(n)=\tfrac{3}{5}\varepsilon_F(n)+\varepsilon_{\rm xc}(n) \ . \quad \text{(B2)}$$

We seek a density $n(x)$ which for $x<\tilde{x}$ is positive and satisfies the Euler equation

$$\delta E/\delta n(x)=g(n)+\phi(x)=\mu \ , \quad \text{(B3)}$$

where

$$g(n)=d[n\varepsilon(n)]/dn \ . \quad \text{(B4)}$$

For $x>\tilde{x}$, $n(x)$ is identically 0 and $g(n)+\phi(x)>\mu$. $E[n]-\mu\int d^3r\, n(\mathbf{r})$ must be minimal with respect to variations of $\tilde{x}$:

$$\frac{d}{d\tilde{x}}\left[E[n]-\mu\int d^3r\, n(\mathbf{r})\right]=0=A[n\varepsilon(n)+n\phi-\mu n]\,|_{\tilde{x}} \ , \quad \text{(B5)}$$

where A is the surface area and, according to (B3),

$$\mu=[g(n)+\phi]\,|_{\tilde{x}} \quad \text{(B6)}$$

is the chemical potential. Substitution of (B6) into (B5) yields

$$\left.\frac{d}{dn}\varepsilon(n)\right|_{\tilde{x}}=0 \ . \quad \text{(B7)}$$

Thus, as x increases, the density $n(x)$ approaches a critical value $n(\tilde{x})=\bar{n}$, the root of Eq. (B7), and then vanishes for $x>\tilde{x}$.

To find the work function for $\bar{n}>\tilde{n}$, note that from (B3)

$$\mu=g(\bar{n})+\phi(-\infty) \ . \quad \text{(B8)}$$

Substracting (B8) from (B6) yields

$$W=\phi(\tilde{x})-\phi(-\infty)-g(\bar{n})=-g(\tilde{n})=-\varepsilon(\tilde{n}) \ . \quad \text{(B9)}$$

Equation (B6) applies not only to a surface but also to a neutral atom:[8,10] $\mu=g(\tilde{n})$ for $\phi(\tilde{x})=0$.

With Ceperley-Alder correlation,[5,6] the critical density $\tilde{n}$ corresponds to a local $\tilde{r}_s=4.18$, and the work function of Eq. (B9) is 2.11 eV, independent of the bulk r_s for $r_s<\tilde{r}_s$. Without correlation (Thomas-Fermi-Dirac approximation), $\tilde{r}_s=4.82$ and $W=1.29$ eV. With neither exchange nor correlation (Thomas-Fermi approximation), $\tilde{r}_s=\infty$ and $W=0$. These are the r_s-independent estimates of the work function from Ref. 9 (with a small difference arising from the use of Wigner correlation in Ref. 9).

In Sec. I of this paper, we propose that the TFDG work function is an estimate of the high-density limit. We now argue that the TFDG approximation becomes increasingly less realistic at lower bulk densities $\bar{n}$. Consider the electron density at the jellium edge $n(0)$. Table II shows $n(0)/\bar{n}$ versus $r_s=(3/4\pi\bar{n})^{1/3}$, as calculated

TABLE II. Ratio $n(0)/\bar{n}$ of the electron density at the jellium edge to that in the bulk. $r_s=(3/4\pi\bar{n})^{1/3}$ is the bulk density parameter. TFD: Thomas-Fermi-Dirac. TFDG: Thomas-Fermi-Dirac-Gombas. KS-X: Kohn-Sham with local exchange alone. KS-XC: Kohn-Sham with local exchange and correlation.

r_s	TFD	TFDG	KS-X	KS-XC
0.5	0.4701	0.4704	0.4651	0.4654
0.75	0.4732	0.4740	0.4654	0.4662
1.0	0.4769	0.4783	0.4656	0.4669
1.5	0.4858	0.4897	0.4611	0.4622
2	0.4980	0.5067	0.4514	0.4512
4	0.6712	0.8818	0.4108	0.4023
6	0	0	0.3802	0.3612
12	0	0	0.3163	0.2607

self-consistently within the Kohn-Sham formalism using local exchange and correlation (XC) or exchange along (X). Shown for comparison are the TFD values of $n(0)/\bar{n}$. In the high-density limit, all three approximations yield $n(0)/\bar{n}=(\frac{3}{5})^{3/2}=0.4648$, which is the TF value for all $\bar{n}$. But the TFD values become increasingly less realistic at lower densities $\bar{n}$.

The TFD values of $n(0)$ have been computed from the following argument. The Budd-Vannimenus theorem of Eq. (13),

$$\phi(0)-\phi(-\infty)=\bar{n}\,d\varepsilon(\bar{n})/d\bar{n}\ , \tag{B10}$$

is true within any self-consistent scheme, including TFD. From Eq. (B3), the TFD density satisfies

$$g(\bar{n})+\phi(-\infty)=\mu\ , \tag{B11}$$

$$g(n(0))+\phi(0)=\mu\ . \tag{B12}$$

Equation (B12) holds so long as $n(0)>0$, i.e., so long as $\tilde{x}>0$. Subtracting (B11) from B(12) and inserting the result into (B10) yields an equation for the TFD value of $n(0)$:

$$g(n(0))=\varepsilon(\bar{n})\ . \tag{B13}$$

Equation (B13) is just a quadratic equation for $n(0)^{1/3}$, and its solution is displayed in Table II. As r_s approaches $\tilde{r}_s=4.82$ from below, the ratio $n(0)/\bar{n}$ approaches unity and $\tilde{x}$ approaches zero. For lower densities ($r_s>\tilde{r}_s$), it appears that $\tilde{x}$ is negative, $n(0)=0$, and

$$W=[\phi(0)-\phi(\tilde{x})]-g(\bar{n})$$
$$=-2\pi\bar{n}\,\tilde{x}^2-g(\bar{n})\ . \tag{B14}$$

Thus, for $r_s>\tilde{r}_s$, the TFD work function begins to fall below its high-density value of $-g(\bar{n})$.

An alternative way to solve for $n(0)/\bar{n}$ is to find the root of Eq. (B13) numerically. This method was checked out on the TFD problem and then applied to the TFDG problem, with the results shown in Table II.

When density-gradient corrections to the kinetic energy are incorporated along with local exchange and correlation (Thomas-Fermi-Dirac-Gombas-Weizsaecker approximation), the work function depends upon the bulk density in a way that may be calculated either variationally[9,15,18] or exactly.[19] In the normal metallic range, this density dependence is qualitatively similar to that of Table I, in which the kinetic energy is treated exactly.

[1]N. D. Lang and W. Kohn, Phys. Rev. B **1**, 4555 (1970).
[2]N. D. Lang and W. Kohn, Phys. Rev. B **3**, 1215 (1971).
[3]W. Kohn and L. J. Sham, Phys. Rev. **140**, A1333 (1965).
[4]L. F. Magaña and M. A. Ocampo, Phys. Rev. B **33**, 7294 (1986).
[5]S. H. Vosko, L. Wilk, and M. Nusair, Can. J. Phys. **58**, 1200 (1980). Essentially the same results would be obtained with the parametrization of J. P. Perdew and A. Zunger, Phys. Rev. B **23**, 5048 (1981).
[6]D. M. Ceperley and B. J. Alder, Phys. Rev. Lett. **45**, 566 (1980).
[7]V. Peuckert, J. Phys. C **7**, 2221 (1974).
[8]P. Gombas, Handb. Phys. **36**, 109 (1956).
[9]J. R. Smith, Ph.D. thesis, Ohio State University, 1968 (unpublished); Phys. Rev. **181**, 522 (1969).
[10]J. W. Sheldon, Phys. Rev. **99**, 1291 (1955).
[11]R. Monnier and J. P. Perdew, Phys. Rev. B **17**, 2595 (1978).
[12]M. Manninen, R. Nieminen, P. Hautojärvi, and J. Arponen, Phys. Rev. B **12**, 4012 (1975).
[13]R. Monnier, J. P. Perdew, D. C. Langreth, and J. W. Wilkins, Phys. Rev. B **18**, 656 (1978).
[14]V. Peuckert, J. Phys. C **9**, 4173 (1976).
[15]J. P. Perdew, Phys. Rev. B **21**, 869 (1980).
[16]V. Sahni, C. Q. Ma, and J. S. Flamholz, Phys. Rev. B **18**, 3931 (1978). See also Ref. 18.
[17]H. F. Budd and J. Vannimenus, Phys. Rev. Lett. **31**, 1218 (1973); **31**, 1430(E) (1973).
[18]C. Q. Ma and V. Sahni, Phys. Rev. B **19**, 1290 (1979).
[19]C. A. Utreras Diaz, Phys. Rev. B **36**, 1785 (1987); A. Chizmeshya and E. Zaremba, *ibid.* **37**, 2805 (1988).